Expression pattern of neuronal and skeletal muscle voltage-gated Na^+ channels in the developing mouse heart

Volker Haufe[1], Juan A. Camacho[1], Robert Dumaine[2], Bernd Günther[3], Christian Bollensdorff[1], Gisela Segond von Banchet[4], Klaus Benndorf[1] and Thomas Zimmer[1]

[1]*Institute of Physiology II, Friedrich Schiller University, 07740 Jena, Germany*
[2]*Masonic Medical Research Laboratory, Utica, NY 13501, USA*
[3]*Institute of Laboratory Animals, Friedrich Schiller University, 07740 Jena, Germany*
[4]*Institute of Physiology I, Friedrich Schiller University, 07740 Jena, Germany*

In the mammalian heart, a variety of voltage-gated Na^+ channel transcripts and proteins have been detected. However, little quantitative information is available on the abundance of each transcript during development, or the contribution of TTX-sensitive Na^+ channels to the cardiac sodium current (I_{Na}). Using competitive and real-time RT-PCR we investigated the transcription of six Na^+ channels ($Na_v1.1$–$Na_v1.6$) and the $\beta1$ subunit during mouse heart development. $Na_v1.5$ was predominantly expressed in the adult heart, whereas the splice variant $Na_v1.5a$ was the major Na^+ channel isoform in embryonic hearts. The TTX-resistant Na^+ channel transcripts ($Na_v1.5$ and $Na_v1.5a$) increased 1.7-fold during postnatal development. Transcripts encoding TTX-sensitive Na^+ channels ($Na_v1.1$–$Na_v1.4$) and the $\beta1$ subunit gradually increased up to fourfold from postnatal day (P)1 to P126, while the $Na_v1.6$ transcript level remained low and constant over the same period. In adults, TTX-sensitive channel mRNA accounted for 30–40% of the channel pool in whole-heart preparations ($Na_v1.3 > Na_v1.4 > Na_v1.2 \gg Na_v1.1 \sim Na_v1.6$), and 16% in mRNA from isolated cardiomyocytes ($Na_v1.4 > Na_v1.3 > Na_v1.2 > Na_v1.1 > Na_v1.6$). Confocal immunofluorescence on ventricular myocytes suggested that $Na_v1.1$ and $Na_v1.2$ were localized at the intercalated disks and in the t tubules. $Na_v1.3$ labelling predominantly produced a diffuse but strong intracellular signal. $Na_v1.6$ fluorescence was detected only along the Z lines. Electrophysiological recordings showed that TTX-sensitive and TTX-resistant Na^+ channels, respectively, accounted for 8% and 92% of the I_{Na} in adult ventricular cardiomyocytes. Our data suggest that neuronal and skeletal muscle Na^+ channels contribute to the action potential of cardiomyocytes in the adult mammalian heart.

(Received 21 November 2004; accepted after revision 1 March 2005; first published online 3 March 2005)
Corresponding author Thomas Zimmer: Friedrich Schiller University, Institute of Physiology II, Teichgraben 8, 07740 Jena, Germany. Email: thomas.zimmer@mti.uni-jena.de

Voltage-gated sodium (Na^+) channels are plasma membrane proteins that mediate the rapid increase in Na^+ permeability during the initial phase of action potentials in electrically excitable cells (Catterall, 1992). During the last 15 years, 10 α and four β subunit isoforms have been cloned from different mammalian tissues (Goldin, 2001; Yu *et al.* 2003).

The $Na_v1.5$ α subunit is highly expressed in the mammalian heart, and is thought to determine the major electrophysiological and pharmacological properties of the sodium current (I_{Na}) in ventricular cardiomyocytes (Balser, 2001; Goldin, 2001) based on similarities to the native current kinetics and low sensitivity to tetrodotoxin (TTX; IC_{50} 0.4–6 μM) (Benndorf *et al.* 1985; Cribbs *et al.* 1990; Satin *et al.* 1992; Nuss *et al.* 1995; Chahine *et al.* 1996). The mouse heart expresses two alternatively spliced variants of $Na_v1.5$, mH1-2 or $Na_v1.5a$, and mH1-3 or $Na_v1.5b$, both with deletions in an intracellular loop (Zimmer *et al.* 2002*b*). $Na_v1.5a$ generates currents indistinguishable from wild-type $Na_v1.5$, whereas $Na_v1.5b$ does not form functional channels. Beside these $Na_v1.5$ transcripts, several TTX-sensitive Na^+ channels (IC_{50} 5–25 nM) have been detected in cardiac RNA preparations, including neuronal $Na_v1.1$ (Rogart *et al.* 1989; Sills *et al.* 1989; Schaller *et al.* 1992; Baruscotti *et al.* 1997; Huang *et al.* 2001), $Na_v1.3$ (Schaller *et al.* 1992; Zimmer *et al.* 2002*b*) $Na_v1.6$ (Sills *et al.* 1989; Pereon *et al.* 2003) and skeletal muscle $Na_v1.4$ (Zimmer *et al.* 2002*b*; Pereon *et al.* 2003). Cardiac expression of $Na_v1.2$ has not yet been reported.

 DOI: 10.1113/jphysiol.2004.079681

Electrophysiological and biochemical studies from 26 years ago provided the first evidence in support of the expression of TTX-sensitive Na^+ channels in the heart. Coraboeuf *et al.* (1979) showed that relatively low concentrations of TTX shortened the action potential of Purkinje fibres and slowed their automatic beating rate. A few years later, Renaud *et al.* (1983), using radioligand binding assays, identified a fraction of TTX-sensitive receptors in plasma membranes of adult rat hearts, suggesting the presence of neuronal or skeletal muscle Na^+ channels in cardiomyocytes. More recently, three groups localized neuronal Na^+ channel isoforms *in situ* using immunocytochemical approaches on cardiac tissues and myocytes from mouse (Malhotra *et al.* 2001; Maier *et al.* 2002) and dog (Haufe *et al.* 2005).

Despite the progress in identifying the molecular basis of the cardiac I_{Na}, important aspects of the expression of the different Na^+ channel isoforms in the heart are poorly understood: Experimental data on the developmental regulation of transcription of the different Na^+ channel isoforms in the heart, on the relative contribution of each individual isoform to the total Na^+ channel mRNA pool, as well as on the portion of functional TTX-sensitive Na^+ channels that contribute to the cardiac I_{Na} are largely unknown. Therefore, in the present study we compared, by a competitive PCR approach and by real-time PCR, the mRNA levels of six individual Na^+ channel isoforms, including the β_1 subunit, during mouse heart development, we investigated by immunofluorescence the *in situ* localization of the channel proteins in adult ventricular cardiomyocytes, and we determined by patch-clamp recordings, the fraction of functional TTX-sensitive Na^+ channels that contribute to the transient I_{Na} of ventricular cardiomyocytes.

Methods

RNA isolation and cDNA synthesis

BALB/c mice were anaesthetized by inhalation of a mixture of 50% O_2 and 50% CO_2, killed by cerebral dislocation at the different developmental stages (postnatal days (P)1, 9, 38, 76 and 126), and hearts were carefully excised. For each time point, we used one mouse heart from the same litter. Embryonic hearts were isolated under a microscope, and four hearts were pooled for RNA isolation. Hearts were rinsed in saline to remove excess blood, and homogenized mechanically with an Ultra-Turrax T8 homogenizer (IKA Labortechnik, Staufen, Germany). Total RNA was prepared according to the acid guanidinium thiocyanate/phenol/chloroform method (Chomczynski & Sacchi, 1987) using the RNAPure· solution (Peqlab Biotechnologie GmbH, Erlangen, Germany). The primary RNA fraction was precipitated twice with 0.8 M LiCl to improve conditions for reverse transcription and PCR (Mathy *et al.* 1996). Reverse transcription was performed using an equimolar mix of the poly-A-anchored oligonucleotides dTAN, dTCN and dTGN, and Superscript II, according to the suggestions of the supplier (Invitrogen, Groningen, The Netherlands), followed by treatment of the cDNA mixture for 20 min at 37°C with *Escherichia coli* RNase H (MBI Fermentas, Vilnius, Lithuania). Animal experimentation was performed in accordance with the guidelines of the Society for Laboratory Animal Science (GV-SOLAS) and the German Law on the Protection of Animals.

Isolation of partial sequences of mouse $Na_v1.1$, $Na_v1.2$ and $Na_v1.3$

At the beginning of this study, overlapping sequences of the mouse brain Na^+ channels $Na_v1.1$, $Na_v1.2$ and $Na_v1.3$ were not available in the GenBank or EMBL databases. To include these α subunit isoforms in our study, we isolated partial cDNA fragments by RT-PCR. First, we created an alignment of the three corresponding rat sequences plus the mouse $Na_v1.4$ and $Na_v1.5$ sequences using the CLUSTAL program of the Lasergene software (DNASTAR, Inc., Madison, USA). Highly homologous regions were selected as the primer sequences for the subsequent amplification by PCR. To minimize PCR errors we used PfuTurbo DNA Polymerase (Stratagene, La Jolla, USA). In our initial experiments, we applied the primer pair A1 (Table 1) to amplify a fragment pool from a brain and a heart cDNA library. Both amplicon pools were subcloned in pUC119 (*Hinc*II site) and five clones of each cDNA were analysed by DNA sequencing. We detected only $Na_v1.2$ in the brain cDNA, and $Na_v1.3$ in the heart cDNA. This suggested that $Na_v1.3$ mRNA levels are lower in brain but higher in heart when compared with $Na_v1.2$. A fragment coding for $Na_v1.1$ was isolated only by using a brain cDNA library and primer pair A2 (Table 1). Classification of the isolated mouse clones as $Na_v1.1$ (accession no. AJ810515), $Na_v1.2$ (accession no. AJ810516) and $Na_v1.3$ (accession no. AJ810517) was done according to their homology with the known sequences of rat and human. Finally, identical nucleotide stretches in the isolated $Na_v1.1$, $Na_v1.2$ and $Na_v1.3$ fragments were selected and used as primers for simultaneous amplification of the three partial Na^+ channel fragments from the respective cardiac cDNA libraries (see Table 1).

Experimental strategy for competitive PCR assays

To compare the transcriptional levels of the cardiac Na^+ channel isoforms during ontogeny, we performed RT-PCR assays with primers that were designed to allow for simultaneous amplification of different Na^+ channel cDNA species in a single reaction. We included the brain-type Na^+ channel isoforms $Na_v1.1$, $Na_v1.2$ and $Na_v1.3$, the nerve-type Na^+ channel $Na_v1.6$, the isoform

Table 1. Primer pairs used for competitive and real-time RT-PCR

Pair	Sequence (5′–3′) of forward/reverse primer	Amplification of	Size (bp)	Coding for
A1	GTCATCATAGACAACTTCAACCAG/GCAGATCATGCTGTTGCCAAAA	$Na_v1.2/1.3$	706	DIII/S6–DIV/S5
A2	GTCATTATCGACAATTTCAACCAG/AGATCAGGCTGATGCCGAAA	$Na_v1.1$	706	DIII/S6–DIV/S5
A3	CCTGTATGCCTCTGGTCG/GTGTTGGCATAGAGGTCTT	β-actin	450	—
A4	ATGGTCATTGGCAACCTTGTGGT/GAAGATGATGAAAGTCTCGAACCA	$Na_v1.5/1.5a/1.5b$	873/714/270	DII/S6–DIII/S1
A5	GCCTTCGAGGACATCTAC/AAGAAGGAGCCGAAGATG	$Na_v1.4/1.5$	710	DIII/S1–DIII/S6
A6	CARAAGAAGAAGTTTGGAGG/GTCTCAAAGTTGAACATGTC	$Na_v1.1/1.2/1.3$	660	DIII/S6-DIV/S5
A7	AACATGGTGACCATGATGGT/GTAGATGAACATGACGAGGAA	$Na_v1.3/1.5$	393	DIV/S1-DIV/S5
A8	AACATGGTGACCATGATGGTGGA/AAGTTGGACATCCCAAAGATGG	$Na_v1.1/1.2/1.3/1.6$	415	DIV/S1–DIV/S5
A9	GAATGTCACGTCTACCGTC/TCGTGGCTCCACTGCAGAACTGT	β1 subunit	453	—
A10	CAAAAAAGCCACAAAAGCCT/TTAGCTCCGCAAGAAACATC	$Na_v1.1$	326	III/IV loop–DIV/S3
A11	CTCGCCCTGCTAACAAGTTT/CCAGGTTGATCCAATACAGG	$Na_v1.2$	164	III/IV loop–DIV/S2
A12	TTGGCTCCAAAAAACCTCAG/TTGAGAGAATCACCACCACA	$Na_v1.3$	306	III/IV loop–DIV/S3
A13	GAGCTGAAAGACAATCA/CTGCTGAGCAAGATCATGAA	$Na_v1.4$	470	II/III loop–DIII/S1
A14	ATGGTCATTGGCAACCTTGTGGT/CTGTTCTCTTCATCCTCTTC	$Na_v1.5$	430	DII/S6–II/III loop
A15	AGAAGAAGTACTACAACGCC/AGTAGTGTCTCAAGGCAAAC	$Na_v1.6$	285	III/IV loop–DIV/S3
A16	TTAACCCCGAGATGCTGAAC/GAATTCTCTGCAGACCTTGG	PGP 9.5	590	—
A17	TGAGAGCTTTCGGGATGCCA/TGTACACAGTCCGACGACAA	ENO2	646	—

R represents G or A (see third position of A6 forward primer).

of skeletal muscle $Na_v1.4$, and the cardiac-specific isoform $Na_v1.5$, including its splice variants $Na_v1.5a$ and $Na_v1.5b$. The limited availability of sequence information and the relative low homology between some of the isoforms did not allow the design of a single primer pair that simultaneously amplified fragments of all these Na^+ channel variants in a single PCR reaction. Instead, we compared in separate reactions the transcriptional levels of the following: (1) wild-type $Na_v1.5$ *versus* splice variants $Na_v1.5a$ and $Na_v1.5b$ (primer pair A4, Fig. 1*A*), (2) the sum of the $Na_v1.5$-derived transcripts *versus* $Na_v1.4$ (primer pair A5, Fig. 1*B*), (3) $Na_v1.1$ *versus* $Na_v1.2$ *versus* $Na_v1.3$ (primer pair A6, Fig. 1*C*), (4) the sum of the $Na_v1.5$ transcripts *versus* $Na_v1.3$ (primer pair A7, Fig. 1*D*), and (5) the sum of $Na_v1.1$, $Na_v1.2$ and $Na_v1.3$ *versus* $Na_v1.6$ (primer pair A8, Fig. 1*E*). This strategy allowed us to compare the expression levels of the different α subunits (summarized in Fig. 2): $Na_v1.5$ levels were directly correlated to levels of $Na_v1.5a$, $Na_v1.3$ and $Na_v1.4$. Transcript levels of $Na_v1.1$ and $Na_v1.2$ were directly correlated to those of $Na_v1.3$, and $Na_v1.6$ levels were adjusted to the sum of $Na_v1.1/Na_v1.2/Na_v1.3$. The values at the specified times were finally normalized with respect to the sum of all transcripts at P126 where the expression level of all Na^+ channels relative to β-actin was the highest.

Competitive PCRs were done with Pfu DNA Polymerase (Promega, Madison, USA) according to the recommendation of the supplier. Cycle conditions were as follows: denaturation at 94°C for 1 min, annealing at 54°C to 64°C for 1.5 min, extension at 72°C for 3 min. The different cDNAs were diluted at least 10-fold. In order to compare the different developmental stages regarding alterations of Na^+ channel transcript levels (1) the same amount of total RNA was used for cDNA preparation, and (2) the cDNA input for each PCR was adjusted to yield identical densitometry values for the β-actin. Please note that data interpretation about time-dependent changes of absolute values were based on the normalization relative to β-actin, and thus on the assumption that β-actin levels do not change significantly during development. Cycle numbers were between 20 and 30. Original PCR products were subject to specific restriction endonuclease treatment to distinguish between the different isoforms. Product quantification was done by determining the fluorescence intensities of bands of interest from an agarose gel with the gel documentation system from Herolab (Wiesloch, Germany). In the present study, we always corrected the respective intensity values according to the product sizes in order to obtain the molar ratios.

Controls for competitive PCR assays

The reliability of the assay conditions was tested by amplification of the Na^+ channel fragments using mixtures of plasmids encoding the corresponding Na^+ channels to determine if individual Na^+ channel fragments were amplified with similar efficiencies. Supplementary Fig. S1 illustrates a respective control experiment for simultaneous $Na_v1.4/Na_v1.5$ amplification with primer pair A5. We tested different molar ratios of plasmids containing the desired Na^+ channel cDNA fragments, and performed PCR only with primer pairs that gave reproducibly the correct molar ratios. We found proportional amplifications for all competitive PCR assays described in this study. We also tested whether or not the relative ratios of the amplicon densities obtained by competitive PCR were independent on the cycle number. Respective ratios were similar when applying <25 cycles

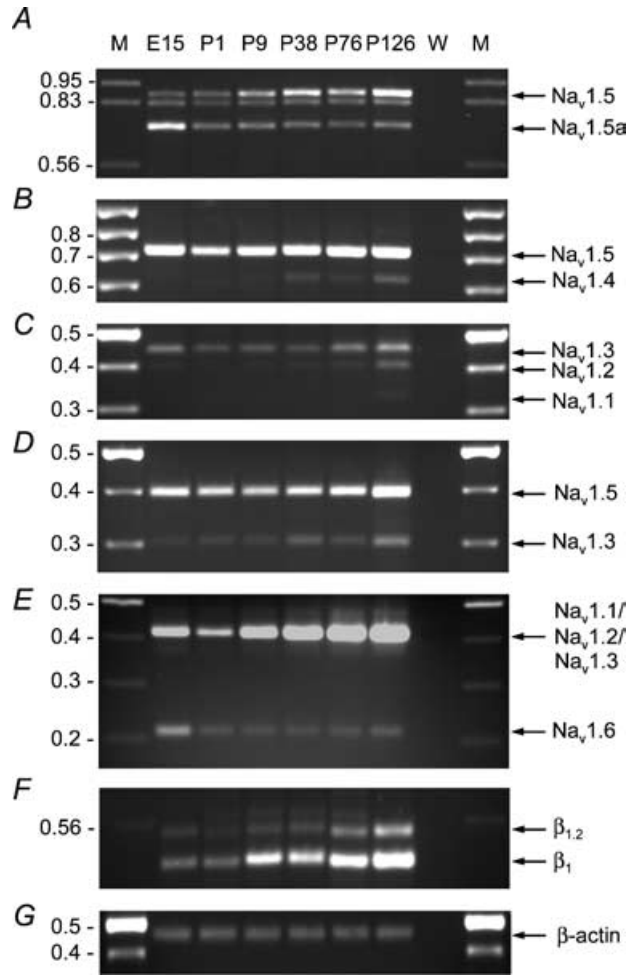

Figure 1. Developmental regulation of Na^+ channel transcription
A, amplification of $Na_v1.5$ and splice variant $Na_v1.5a$. The band between $Na_v1.5$ and $Na_v1.5a$ was composed of a $Na_v1.5$/$Na_v1.5a$ mixture and represented a heteroduplex between both isoforms, similarly as found for other splice variants (Zacharias *et al.* 1994). *B*, developmental regulation of $Na_v1.4$ and $Na_v1.5$ transcription. $Na_v1.4$-specific restriction digestion (*Pvu*II) released a 0.64 and 0.07 kb fragment from the original amplicon (0.71 kb). The $Na_v1.5$ fragment remained undigested at 0.71 kb. In control experiments, the original PCR amplicon was digested with *Pst*I specific for $Na_v1.5$, as illustrated in Fig. S1*A*. *C*, developmental regulation of $Na_v1.1$, $Na_v1.2$ and $Na_v1.3$ transcription. The original PCR amplicons at 660 bp containing $Na_v1.1$, $Na_v1.2$ and $Na_v1.3$ fragments were digested with *Aci*I to release a $Na_v1.1$ fragment at 325 bp (not visible in the picture at early stages but detectable by densitometry), a $Na_v1.2$ fragment at 404 bp, and a $Na_v1.3$ fragment at 454 bp. *D*, developmental regulation of $Na_v1.3$ and $Na_v1.5$ transcription. $Na_v1.3$-specific digestion of the original product (393 bp) with *Bse*NI released 299 and 94 bp fragments. The $Na_v1.5$ fragment remained undigested. In parallel experiments, we proved that the same $Na_v1.5$/$Na_v1.3$ ratios were obtained when specifically digesting only $Na_v1.5$ with *Pvu*II (not shown). *E*, developmental regulation of $Na_v1.6$ transcription. The original PCR product was digested with *Eco*RV to release smaller $Na_v1.6$ fragments at 207 and 208 bp. The other three neuronal Na^+ channel amplicons ($Na_v1.1$, $Na_v1.2$ and $Na_v1.3$) remained at 415 bp. The figure clearly illustrates the strong upregulation of the sum of the $Na_v1.1$, $Na_v1.2$ and $Na_v1.3$ transcripts, whereas $Na_v1.6$ levels were similar at all postnatal time points investigated. *F*, developmental upregulation of the $\beta1$ subunit and splice variant $\beta1.2$ transcription. *G*, the amount of cDNA used in *A*–*F* at the different developmental stages was normalized relative to the amplification of β-actin. M, marker; W, water control (no cDNA added); E15, embryonic day 15; P1–P126, postnatal days 1–126. Please note that primers used in *B* and *D* did not us allow to distinguish between the different $Na_v1.5$ variants.

(~20% of maximal amplicon density) or >30 cycles (40–100% of maximal amplicon density), suggesting competitive conditions for all simultaneously amplified fragments. An example of such a PCR control reaction is shown in supplementary Fig. S1B. The experiment illustrates that the competitive conditions in the same tube (e.g. primer and nucleotide availability, polymerase activity and buffer conditions) applied for all fragments in this tube. Please note that all competitive amplifications using heart cDNAs were terminated when 15–25% of the saturation level was reached. To visualize bands with a lower fluorescence, we applied a respective larger amount of the PCR product on the agarose gel. Breeding and the following heart cDNA preparations were repeated as follow: twice for E15, P1 and P9, five times for P38, three times for P76, and twice for P126. All competitive PCRs were repeated at least twice for each cDNA.

Transcript quantification with LightCycler RT-PCR (real-time RT-PCR)

Real-time RT-PCR was carried out using the LightCycler from Roche (Mannheim, Germany) in combination with the QuantiTect SYBR Green PCR Kit from Qiagen (Hilden, Germany). Master mixes were prepared by following the manufacturer's instructions, using the specific primer pairs listed in Table 1 (A10–A15 for the individual Na^+ channels; A9 for the $\beta1$ subunit). The following temperature profile was used for amplification: denaturation/activation for 1 cycle at 95°C for 15 min, and 45 cycles at 95°C for 1 min (temperature transition, 20°C s^{-1}), 54–64°C for 1 min (temperature transition, 20°C s^{-1}), and 72°C for 1–2 min (temperature transition, 3°C s^{-1}) with fluorescence acquisition at 54–64°C in single mode. Melting curve analysis was done at 45–95°C with stepwise fluorescence acquisition. The specificity of all PCR reactions was verified by ethidium bromide staining of the original product on a 1% agarose gel, and by specific restriction endonuclease treatment. Sequence-specific standard curves were generated using 10-fold serial dilutions (10^{-6}- to 10^{-10}-fold) of plasmids containing cloned cDNA fragments of the individual Na^+ channel subunits. The concentration of all plasmid preparations was carefully adjusted to 1 $\mu g\,\mu l^{-1}$ prior to the dilution step. This equalization was necessary to compare the amplicon levels obtained for the individual Na^+ channel α subunits and to determine the $\alpha/\beta1$ stoichiometry.

Isolation of mouse ventricular cardiomyocytes

Only freshly dissociated ventricular cardiomyocytes were used for electrophysiological measurements, RNA isolation and immunohistochemistry. Ventricular cardiomyocytes for patch-clamp recordings and RNA isolation were obtained according to a previously described standard procedure (Benndorf, 1993). Ventricular cardiomyocytes for immunolabelling experiments were prepared as follows: heparin (0.05 ml, 5000 U ml^{-1}) and pentobarbital sodium (0.03 ml, 64.8 mg ml^{-1}) were injected peritoneally 10 min prior to cerebral dislocation and excision of the heart. The excised heart was transferred to a dish containing Ca^{2+}-free dissecting solution (mM: 140 NaCl, 5.8 KCl, 0.5 KH_2PO_4, 0.4 Na_2HPO_4, 0.9 $MgSO_4$, 11.1 glucose, 10 Hepes, 20 2,3-butanedione monoxime, pH 7.1, NaOH), and perfused using a Langendorff setup at 32°C for 5 min with Ca^{2+}-free dissecting solution, and for 12 min with enzyme solution containing Ca^{2+}-free dissecting solution and 35 U ml^{-1} collagenase (Worthington Enzyme Type II, 237 U mg^{-1}) and 1% BSA (Sigma). Ventricles were cut and minced in enzyme solution for at least 5 min. Quality of the myocytes as judged by the intensity of the Z lines, an indicator of hypercontraction and cell death, was assessed by phase-contrast microscopy. Hypercontracted myocytes were readily identifiable by their rounded ends, their general curved shape, and numerous very tight and dark lines on their surface. Relaxed and thus viable myocytes, on the other hand, had square edges and were fairly rectangular. After cell sedimentation on ice, the enzyme solution was removed and substituted by Ca^{2+}-free Tyrode containing (mM): 120 NaCl, 10 Hepes, 3.3 $MgSO_4$, 2.5 KCl, 1 $MgCl_2$, 2 EGTA, pH 7.4, NaOH. In instances were the yield of viable cells was low, the fraction was enriched by purification on a Percoll gradient as previously described (Heathers *et al.* 1987; Zimmer *et al.* 2002*a*). A ratio of 70% viable cells was deemed adequate to carry out the immunodetection procedure.

Immunocytochemistry

The $Na_v1.1$, $Na_v1.2$ and $Na_v1.3$ antibodies were purchased from Alomone Laboratories (Israel). These antibodies are directed against a short variable region within the intracellular loop between domains I and II of the respective α subunit (residues 465–481 of $Na_v1.1$, accession no. P04774; residues 467–485 of $Na_v1.2$, accession no. P04775; residues 511–524 of $Na_v1.3$, accession no. P08104). Specific localization of $Na_v1.5$ was obtained using a polyclonal $Na_v1.5$ antibody raised in rabbits, and directed against a synthetic oligopeptide corresponding to the epitope PQVRASDYSRSEDLAD unique to the COOH-terminal region of $Na_v1.5$ (Haufe *et al.* 2004). In immunoblots, we confirmed that the antibody recognized a major band at nearly 220 kDa, and that this band was specific for the unique $Na_v1.5$ epitope. Furthermore, we also tested the $Na_v1.5$-specific antibody from Chemicon International, Inc. (Temecula, CA, USA; residues 493–511 of $Na_v1.5$, accession no. P15389) and found very similar results. The $Na_v1.6$ antibody was obtained from Chemicon International, Inc. The respective epitope corresponds to a region within the intracellular loop between domains II and III (residues 1042–1061, accession no. AAC26014). We confirmed the results obtained for $Na_v1.2$ using three different antibody batches from Alomone Laboratories.

Fixation and permeabilization of single ventricular myocytes was done as previously described (Zimmer *et al.* 2002*a*). Rabbit primary antibodies (1:100 or 1:200) were applied overnight at 4°C in a humid chamber, and detected with a goat antirabbit antibody (1:1000) conjugated to the green fluorescent dye Alexa 488 (Molecular Probes, USA). Propidium iodine (PI) was used to stain nucleotide-rich regions (nucleus). Cells were mounted using Pro-Long antifade mounting media (Molecular Probes), and visualized under confocal microscopy using an Olympus Fluoview (Olympus, Japan) as previously described (Zimmer *et al.* 2002*a*).

Heterologous expression in HEK293 cells

HEK293 cells were cultured in MEM (Gibco BRL) supplemented with 10% fetal bovine serum, 2 mM glutamine, 100 U ml^{-1} penicillin, 100 μg ml^{-1} streptomycin and 0.25 μg ml^{-1} amphotericin B. Cells were transfected by a standard calcium phosphate precipitation method using 1–2 μg plasmid DNA per transfection (60 mm cell culture dishes; for the $Na_v1.5$ expression

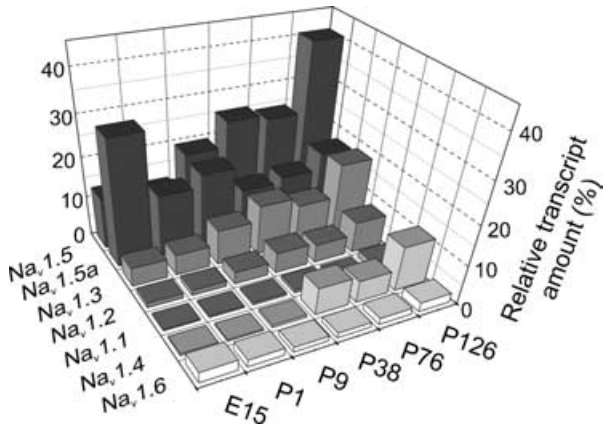

Figure 2. Summary of the developmental regulation of transcription of $Na_v1.1$–$Na_v1.6$ in the mouse heart
The data points were obtained from different competitive PCR assays as presented in Fig. 1. Individual values and standard deviations are presented in Table 2. The relative intensities of the bands obtained for each specific restriction digest, as presented in Fig. 1 and Table 2, were averaged and normalized as described in Methods. Please note that time-dependent changes of transcript levels are presented as amplicon densities relative to β-actin.

Table 2. Relative transcript levels of Na^+ channels determined by competitive RT-PCR

		Relative transcript level at stage					
Primer pair	Amplified Na_v	E15	P1	P9	P38	P76	P126
A4	1.5	0.22 ± 0.02	0.21 ± 0.04	0.34 ± 0.02	0.44 ± 0.02	$0.42 \pm 0.03^{**}$	$0.69 \pm 0.02^{***}$
	1.5a	0.53 ± 0.05	$0.27 \pm 0.05^{*}$	0.32 ± 0.01	0.21 ± 0.01	0.23 ± 0.02	0.31 ± 0.01
A5	1.4	0.01 ± 0.01	0.01^{a}	0.01^{a}	0.10 ± 0.02	$0.07 \pm 0.02^{**}$	0.16 ± 0.03
	1.5	1.01 ± 0.07	$0.43 \pm 0.09^{*}$	0.69 ± 0.06	0.57 ± 0.11	$0.79 \pm 0.12^{**}$	$0.84 \pm 0.07^{***}$
A6	1.1	0.03^{b}	0.02^{b*}	0.02^{b}	0.02^{b}	0.03^{b**}	$0.06 \pm 0.01^{***}$
	1.2	0.09 ± 0.01	0.06^{b*}	0.09 ± 0.01	0.12 ± 0.01	$0.16 \pm 0.02^{**}$	$0.31 \pm 0.04^{***}$
	1.3	0.28 ± 0.01	0.22 ± 0.02	0.25 ± 0.01	0.30 ± 0.01	$0.41 \pm 0.01^{**}$	$0.63 \pm 0.05^{***}$
A7	1.3	0.07 ± 0.01	0.08 ± 0.01	0.10 ± 0.01	0.14 ± 0.04	$0.13 \pm 0.01^{**}$	$0.24 \pm 0.01^{***}$
	1.5	0.71 ± 0.08	$0.46 \pm 0.02^{*}$	0.44 ± 0.04	0.45 ± 0.11	$0.57 \pm 0.04^{**}$	$0.76 \pm 0.02^{***}$
A8	1.1/1.2/1.3	0.14 ± 0.01	0.11^{a*}	0.21 ± 0.02	0.42 ± 0.07	$0.65 \pm 0.06^{**}$	$0.96 \pm 0.01^{***}$
	1.6	0.07 ± 0.02	0.03^{b*}	0.02^{a}	0.02^{a}	0.03^{a}	0.04^{a}

For each primer pair, intensities determined from the respective agarose gels were normalized with respect to the sum of all amplicons at P126. For normalization of the amount of different cDNAs we used β-actin as an internal standard (see Fig. 1*G*). Data are presented as means ± S.E.M. For number of measurements see Methods. Representative agarose gels are shown in Fig. 1. $^{*}P < 0.05$ for E15 *versus* P1; $^{**}P < 0.05$ for P1 *versus* P76; $^{***}P < 0.05$ for P38 *versus* P126. ^{a}S.E.M. $< \pm 0.006$; ^{b}S.E.M. $< \pm 0.002$.

plasmid see Zimmer *et al.* 2002*b*). After an incubation time of 24 h, the transfection mixture was removed, and the cells were seeded onto poly-L-lysine-coated glass coverslips and cultured in fresh growth medium. Currents were investigated 24–48 h after transfection.

Electrophysiological measurements

All recordings were performed with the patch-clamp technique on the stage of an inverted microscope (Axiovert 100, Carl Zeiss Jena GmbH, Germany) using an Axopatch 200B amplifier (Axon Instruments, Foster City, USA). The measurements were carried out at room temperature. Glass pipettes were pulled from borosilicate glass, and their tips were heat polished by the microforge MF 830 (Narishige, Japan). The pipette resistance was between 1.5 and 2.5 MΩ when filled with the pipette solution (mM): 10 Hepes, 10 EGTA, 139 CsCl, 1 NaCl, pH 7.35 (cardiomyocytes); and 10 Hepes, 10 EGTA, 130 CsCl, 10 NaCl, pH 7.35 (HEK293 cells). The bath solution contained (mM): 10 Hepes, 10 glucose, 137 CsCl, 3 NaCl, 1 $MgCl_2$, 0.25 $CaCl_2$, pH 7.35 (cardiomyocytes); and 10 Hepes, 10 glucose, 110 CsCl, 30 NaCl, 1 $MgCl_2$, 0.25 $CaCl_2$, pH 7.35 (HEK293 cells). The Na^+ concentrations were set to a low value to reduce the current amplitude and thus to improve the control of voltage.

The currents were first elicited by test potentials from −120 to 40 mV in 10 mV increments at a pulsing frequency of 0.2 Hz to assess the clamp quality. We used only cells that produced a peak current amplitude <5 nA. Series resistance compensation was adjusted so that any oscillations were avoided, leaving at most 25% of the series resistance uncompensated. We applied test potentials to −50 and −5 mV for 20 ms (holding potential of −120 mV, pulsing frequency of 0.2 Hz) until the current amplitude remained constant at both potentials. Then, we investigated the TTX effect. The toxin was purchased from Biotrend Chemikalien GmbH (Köln, Germany) as the citrate salt and dissolved in water (stock solution, 1 mM). Currents were on-line filtered with a cut-off frequency of 10 kHz (four-pole Bessel). Recording and analysis of the data were performed on a personal computer with the ISO2 software (MFK, Niedernhausen, Germany). The sampling rate was 50 kHz.

Results

Developmental expression pattern of $Na_v1.1$–$Na_v1.6$ in the mouse heart

We first compared $Na_v1.5$ *versus* $Na_v1.5a$ levels at different stages of development. Figure 1*A* shows that the amount of $Na_v1.5$ transcripts gradually increased during ontogeny, while $Na_v1.5a$ mRNA was abundant at the embryonic stage, but decreased rapidly after birth and remained at a constant level up to P126 (Table 2). The total amount of transcripts for TTX-resistant channels ($Na_v1.5 + Na_v1.5a$) increased 1.7-fold between P1 and P126. The molar ratio of $Na_v1.5$ to $Na_v1.5a$ was about 1:2.5 at embryonic day (E)15, but was nearly reversed in the adult heart (P38–P126). These results indicate that the $Na_v1.5a$ splice variant is the predominant Na^+ channel isoform in embryonic hearts. The primer pair specific for amplification of $Na_v1.5$ and $Na_v1.5a$ simultaneously produced a faint 270 bp band after 40 PCR cycles, corresponding to splice variant $Na_v1.5b$. The intensity of this band was similar at all stages (<3% of $Na_v1.5$; data not shown). Our data indicate that the $Na_v1.5$ variants are differentially expressed during ontogeny, with the alternatively spliced $Na_v1.5a$ transcripts significantly downregulated at birth, but not modulated in an age-dependent manner afterwards.

Transcripts of $Na_v1.4$ were absent or present at very low levels before birth and until P9 (Fig. 1*B*, Table 2). From P9 to P126, $Na_v1.4$ transcription increased to give a maximum fluorescence intensity corresponding to 20% of that observed for $Na_v1.5$, with ratios of 0.84 and 0.16 of total amplicon intensity for $Na_v1.5$ and $Na_v1.4$, respectively.

Using primer pair A6 (Table 1) we found that simultaneous amplification of $Na_v1.1$, $Na_v1.2$ and $Na_v1.3$ yielded a gradual increase in signal as the mouse is ageing (Fig. 1*C*). Specific restriction digestion of $Na_v1.1$, $Na_v1.2$ or $Na_v1.3$ revealed that $Na_v1.3$ was the major neuronal Na^+ channel transcript at all developmental stages (Table 2), and that it increased threefold from P1 to P126. $Na_v1.2$ expression was barely detectable up to P38, from where it gradually increased to account for 31% of the total amplicon intensity at the late adult stage P126. Fluorescence signals corresponding to $Na_v1.1$ were slightly above background at all developmental stages, accounting for a maximum of 6% of the total signal at P126 (Table 2).

To estimate the expression levels of these brain Na^+ channels relative to those of $Na_v1.5$, we performed a competitive PCR using primer pair A7 that simultaneously amplified $Na_v1.3$ and $Na_v1.5$ (including $Na_v1.5a$ and $Na_v1.5b$). Relative levels of each Na^+ channel isoform were analysed by specific restriction digestion (Fig. 1*D*, Table 2). As expected, $Na_v1.5$ was the predominant isoform at all stages investigated (76% $Na_v1.5$ *versus* 24% $Na_v1.3$ at P126). Both Na^+ channels were upregulated similarly after birth, as shown in Fig. 1*A*–*C*.

Co-amplification of $Na_v1.6$, $Na_v1.1$, $Na_v1.2$ and $Na_v1.3$ with primer pair A8 showed that $Na_v1.6$ transcripts were more abundant at the embryonic stage, but that expression was strongly reduced and reached a steady-state level immediately after birth (Fig. 1*E*). The amount of combined $Na_v1.1$, $Na_v1.2$ and $Na_v1.3$ transcripts slightly decreased from E15 to P1, and gradually increased during postnatal development (Table 2). Our results therefore show that $Na_v1.6$ mRNA is much less abundant when compared with $Na_v1.2$ and $Na_v1.3$.

The relative contribution of each Na^+ channel transcript to the genetic makeup of the cardiac Na^+ current is summarized in Fig. 2. Our results indicate that $Na_v1.5a$, $Na_v1.5$ and $Na_v1.3$ transcripts are the main mRNA types present during the embryonic stage. $Na_v1.1$ and $Na_v1.6$ mRNA remained rare at all developmental stages, while $Na_v1.2$, $Na_v1.3$, $Na_v1.4$ and $Na_v1.5$ transcripts gradually increased during development. The transcript pool of TTX-sensitive channels increased from ∼19% in the embryonic and juvenile hearts (E15–P9) to ∼40% in the adult heart in the order $Na_v1.3 > Na_v1.4 > Na_v1.2 \gg Na_v1.1 \sim Na_v1.6$. The isoforms $Na_v1.2$, $Na_v1.3$ and $Na_v1.4$ constituted more than 90% of the sum of all TTX-sensitive channel transcripts.

Table 3. Relative expression levels of different Na^+ channels in mouse heart and in isolated ventricular myocytes (stage P38)

	Relative amount of mRNA (%)		
$Na_v1.x$	Whole-heart competitive RT-PCR	Whole-heart real-time PCR	Ventricular myocytes real-time PCR
$Na_v1.1$	1.3 ± 0.1	1.4 ± 0.2	0.2 ± 0.1
$Na_v1.2$	7.6 ± 0.7	6.6 ± 0.3	1.0 ± 0.2
$Na_v1.3$	18.8 ± 5.2	14.8 ± 1.5	3.6 ± 1.1
$Na_v1.4$	10.3 ± 2.4	6.7 ± 0.5	10.7 ± 2.2
$Na_v1.5$	60.7 ± 11.5	69.7 ± 4.1	84.4 ± 4.4
$Na_v1.6$	1.3 ± 0.3	0.8 ± 0.3	0.1 ± 0.02

$Na_v1.5$ levels include those for $Na_v1.5a$. Data are means ± S.E.M.

We next validated our competitive PCR approach by comparing the relative transcript levels of $Na_v1.1$ to $Na_v1.6$ at P38 with results obtained in real-time RT-PCR. Table 3 shows that both methods gave similar results.

Expression of the β1 subunit and determination of the α/β1 stoichiometry

Since neuronal Na^+ channels coassemble with the β1 subunit, we tested for its presence in mouse heart. Competitive PCR using primer pair A9 showed that the β1 subunit was upregulated during ontogeny (Fig. 1*F*) with a ∼fourfold increase from E15 and P1 to P126. In addition to the expected 453 bp band, we observed a 540 bp fragment (Fig. 1*F*). The coding sequence of this larger fragment revealed that it belonged to the β1.2 subunit previously described by Dib-Hajj & Waxman (1995). The fragment shared an identical coding sequence with β1 and still contained intron 5 a few base pairs downstream of the stop codon. To our knowledge, the physiological role of intron 5 is still unknown. The RNA ratio between β1 and β1.2 remained relatively constant at all developmental stages, thus excluding the possibility that splicing of intron 5 is developmentally regulated in the heart.

Using real-time RT-PCR and respective external standard curves we next determined the stoichiometry of β1 (plus β1.2) relative to $Na_v1.5$ at P38. In whole heart, the ratio of $Na_v1.5$ to β1 was 1:1.67. Since $Na_v1.5$ mRNA accounts for 60–70% of all Na^+ channel transcripts in the heart (see Table 3), these values indicate nearly equimolar amounts of all Na^+ channel α and β1 transcripts in mouse heart.

Transcript levels of $Na_v1.1$–$Na_v1.6$ in isolated ventricular cardiomyocytes

Because of the small size of embryonic and newborn hearts of mice, and the resulting technical limitations of accurately isolating myocytes from different heart regions,

such as cells from atria, Purkinje fibres or ventricles, we followed the developmental expression patterns only in whole-heart RNA preparations (see Figs 1 and 2). To get first insight into the tissue-specific expression of the six individual Na^+ channel isoforms within the myocardium, we performed real-time RT-PCR on mRNA isolated from freshly dissociated ventricular cardiomyocytes of adult mouse hearts (P38). We found that the amount of neuronal Na^+ channel transcripts relative to $Na_v1.5$ was lower in isolated cardiomyocytes than in whole-heart preparations accounting for 4.9% and 23.6% of the total mRNA pool, respectively (Table 3). Surprisingly, the $Na_v1.4$ mRNA level was higher in ventricular cardiomyocytes (real-time PCR: 10.7% in cardiomyocytes *versus* 6.7% in the whole heart).

Possible contribution of neuronal Na^+ channels from cardiac nerve fibres

Even after carefully dissecting a mouse heart, respective RNA preparations may contain an RNA fraction derived from remaining efferent and afferent nerve fibres innervating the heart. These neuronal cells and respective Schwann cells could be an additional source of Na^+ channel RNA. Because of the difficulties in isolating the ensemble of the cardiac nerve fibres, we used an indirect approach to assess the contribution of neuronal tissues in our cardiac RNA preparations. We first investigated the expression levels of two functionally unrelated neurone-specific markers, of the neuronal ubiquitin carboxyl-terminal hydrolase (PGP 9.5) and of the neuronal enolase 2 (ENO2; Day, 1992), both in the whole heart and in two different neuronal reference tissues, in sympathetic ganglia and in the sciatic nerve. Thus, a high level of these markers in our cardiac RNA preparations relative to their level in neuronal cells would suggest a significant contamination of our whole-heart RNA preparations with RNA from cardiac nerve fibres.

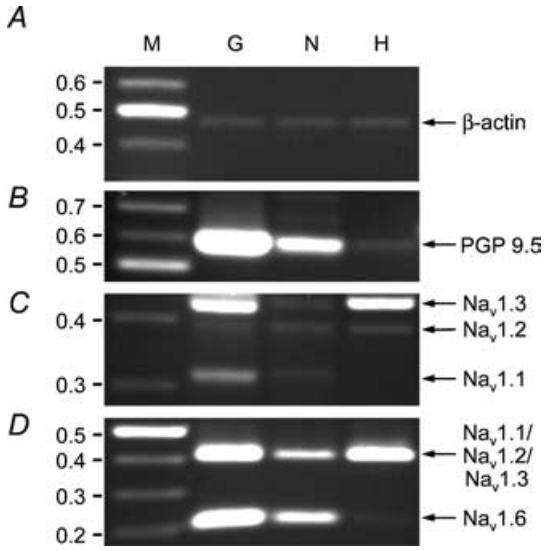

Figure 3. Expression of neuronal Na^+ channels in sympathetic ganglia (G), sciatic nerve (N) and heart tissues (H; P76)
A, amplification of internal standard β-actin. *B*, amplification of neurone-specific marker ubiquitin carboxyl-terminal hydrolase (PGP 9.5). *C*, amplification of neuronal $Na_v1.1$, $Na_v1.2$ and $Na_v1.3$. Specific digestion with *Aci*I of the original PCR product (660 bp) obtained with primer pair A6 revealed the contribution of the individual isoforms. In clear contrast to neurone-specific PGP 9.5, $Na_v1.2$ and $Na_v1.3$ levels were similar or even higher in the whole heart *versus* nerve or ganglia. However, levels of $Na_v1.1$ were highest in ganglia and sciatic nerve, but often only merely above the level detectable by densitometry in the heart samples. *D*, simultaneous amplification of $Na_v1.1$, $Na_v1.2$, $Na_v1.3$ and $Na_v1.6$ (primer pair A8). The original PCR product pool was digested with *Eco*RV to release smaller $Na_v1.6$ fragments at 207 and 208 bp, as described in Fig. 1. In contrast to $Na_v1.2$ and $Na_v1.3$, transcript levels of $Na_v1.6$ were much lower in the heart compared with both neuronal tissues.

To test for respective PGP 9.5 and ENO2 transcript levels, we first normalized the amount of whole heart, sympathetic ganglia and sciatic nerve cDNAs using β-actin as a standard for comparison and indicator of loading errors (Fig. 3*A*). We found that PGP 9.5 levels (Fig. 3*B*, Table 4) were, respectively, >100-fold and $\sim$10-fold higher in ganglia and sciatic nerve when compared with levels found in the heart. Similar data were obtained for the second marker ENO2 (Table 4). These results suggest that, depending on the neuronal reference tissue, cardiac neurones account for less than 1% or at most 10% of the RNA fraction in whole-heart preparations.

Despite the low abundance of PGP 9.5 in our whole-heart preparation, expression of $Na_v1.2$ and $Na_v1.3$ relative to β-actin was still significant (Fig. 3*C*, Table 4). Neither the neuronal cell bodies of the sympathetic ganglia nor the axons and Schwann cells of the sciatic nerve contained higher levels of $Na_v1.2$ and $Na_v1.3$ than the myocardium. This suggests that, despite their detectable expression in the peripheral nerve system, $Na_v1.2$ and $Na_v1.3$ transcripts predominantly occur in cardiac muscle cells. In contrast to this, $Na_v1.1$ and $Na_v1.6$ transcripts (Fig. 3*C* and *D*) were abundant in both neuronal tissues and less expressed in the heart (Table 4), suggesting a contribution of $Na_v1.1$ and $Na_v1.6$ mRNA from neuronal tissues within the heart. However, considering the low levels of $Na_v1.1$ and $Na_v1.6$ in the heart at all developmental stages, even a high degree of such a contamination would not dramatically alter the relative contribution of all individual Na^+ channel isoforms to the total Na^+ channel pool in the heart (see Fig. 2).

Immunolocalization of $Na_v1.1$, $Na_v1.2$, $Na_v1.3$, $Na_v1.5$ and $Na_v1.6$ channels in single cardiomyocytes

To investigate whether or not the different Na^+ channel proteins are produced by ventricular cardiomyocytes, and to determine their subcellular localization, we incubated freshly dissociated ventricular cardiomyocytes from adult

Table 4. Expression of neuronal markers PGP 9.5 and ENO2, and different Na^+ channels in the adult mouse heart (P76) relative to their expression in ganglia and sciatic nerve

	Transcript ratio	
Transcript	heart *versus* ganglia	heart *versus* nerve
PGP 9.5	<0.01	0.1
ENO2	0.01	0.1
$Na_v1.1$	0.05	0.13
$Na_v1.2$	2.1	1.7
$Na_v1.3$	1.1	8.1
$Na_v1.6$	0.03	0.14

mouse hearts (stage P38) with specific antibodies against $Na_v1.1$, $Na_v1.2$, $Na_v1.3$, $Na_v1.5$ and $Na_v1.6$, and visualized the fluorescent cells by laser scanning microscopy (Fig. 4). A specific antibody against $Na_v1.4$ was not available.

Using the $Na_v1.5$ antibody (Fig. 4*A*), we observed fluorescent structures, similarly as reported previously by Cohen (1996) for rat ventricular cardiomyocytes. Our data also suggest the following: (1) a nearly uniform surface membrane labelling; (2) localization in t tubules, as suggested from staining of parallel lines throughout the cell resembling a Z line staining typical for α-actinin; and (3) staining at the regions of cell-to-cell contact, the intercalated disks. $Na_v1.1$ and $Na_v1.2$ were primarily located at the intercalated disks, but also present along the Z lines (Fig. 4*B* and *C*), similarly as found for $Na_v1.5$. In contrast, $Na_v1.3$ labelling was diffuse throughout the cytoplasm in most cells (Fig. 4*D*). Some cells showed, in addition to the strong intracellular diffuse signal, a dotted-like fluorescence along the Z lines. The $Na_v1.6$ antibody produced fluorescence only along the Z lines (Fig. 4*E*). In control experiments, antibodies preabsorbed overnight against their respective antigen did not yield specific fluorescent signals.

TTX-sensitive Na^+ currents in cardiomyocytes

In order to examine whether or not the TTX-sensitive channels are functionally expressed, we determined the TTX blocking curve of single mouse ventricular cardiomyocytes at the test potentials of −50 and −5 mV by using the whole-cell patch-clamp technique. At −50 mV, the TTX-resistant $Na_v1.5$ channels are already activated, whereas TTX-sensitive Na^+ channels are still closed because they activate at more depolarized potentials (Benndorf *et al.* 1985; Auld *et al.* 1988; Nuss *et al.* 1995; Chahine *et al.* 1996; Smith & Goldin, 1998; Zimmer *et al.* 2002*b*). At −5 mV, all channels are fully activated. If cardiomyocytes contain a TTX-sensitive current component, both blocking curves should be different with a pronounced deviation at relatively low [TTX]. All cells that produced a time-dependent shift of steady-state activation were not further considered.

The results of our measurements are shown in Fig. 5 and Table 5. We found that in the majority of the cells, a significantly larger fraction of Na^+ channels was blocked at −5 mV compared to −50 mV when applying [TTX] between 5 and 50 nM (see Fig. 5*A* and *B*). This differential effect of TTX was not due to a voltage-dependent $Na_v1.5$ block because heterologously expressed $mNa_v1.5$ channels exhibited an indistinguishable block at both potentials (Fig. 5*C*). It must be emphasized, however, that nearly 30% of the cells produced a negligible or even no effect. To emphasize this cell-to-cell variability among ventricular cardiomyocytes, we analysed our measurements both by including all cells independent of whether or not an effect at low [TTX] was observed, and by considering only such cells that showed a clearly detectable TTX-sensitive response (TTXs cells). Assuming a TTX binding to its receptor of 1:1, the TTX concentration of half-maximal block of the TTX-resistant channels ($IC_{50/TTXr}$) in cardiomyocytes was determined by fitting the data points at −50 mV by a Langmuir absorption isotherm:

$$I_{Na,TTX}/I_{Na,control} = 1/\left(1 + [TTX]/IC_{50/TTXr}\right) \quad (1)$$

yielding a value of 399 nM. This value was in good agreement with the IC_{50} of $mNa_v1.5$ channels in HEK293 cells (335 nM; Fig. 5*C*). Using the $IC_{50/TTXr}$ value of 399 nM, and keeping the assumption of a 1:1 binding of TTX to its receptor, the data points at −5 mV for all cells or TTXs cells only were fitted with the sum of two Langmuir absorption isotherms:

$$\begin{aligned} I_{Na,TTX}/I_{Na,control} = {} & \\ & P_{TTXs}\{1/(1 + [TTX]/IC_{50/TTXs})\} \\ & + (1 - P_{TTXs})\{1/(1 + [TTX]/IC_{50/TTXr})\} \end{aligned} \quad (2)$$

yielding an IC_{50} of the TTX-sensitive current ($IC_{50/TTXs}$) of ~11 nM, and a portion of the TTX-sensitive Na^+ current (P_{TTXs}) of 7.9% (all cells) and of 11.3% (TTXs cells).

In conclusion, our data show (1) that most of the isolated ventricular cardiomyocytes contain a small fraction of functional TTX sensitive Na^+ channels, and (2) that these channels are indeed activated at more depolarized potentials with respect to the TTX-resistant channels in their native environment.

Discussion

In the present study, we show that the TTX-resistant Na^+ channel transcripts $Na_v1.5$ plus $Na_v1.5a$ account for nearly 70 and 84% of all Na^+ channel transcripts in the whole heart and in ventricular myocytes, respectively. These results are consistent with a high protein level needed to generate the bulk of the cardiac I_{Na} and the similar electrophysiological properties between heterologously expressed $Na_v1.5$ channels and the native I_{Na} (Cribbs *et al.* 1990; Satin *et al.* 1992; Nuss *et al.* 1995).

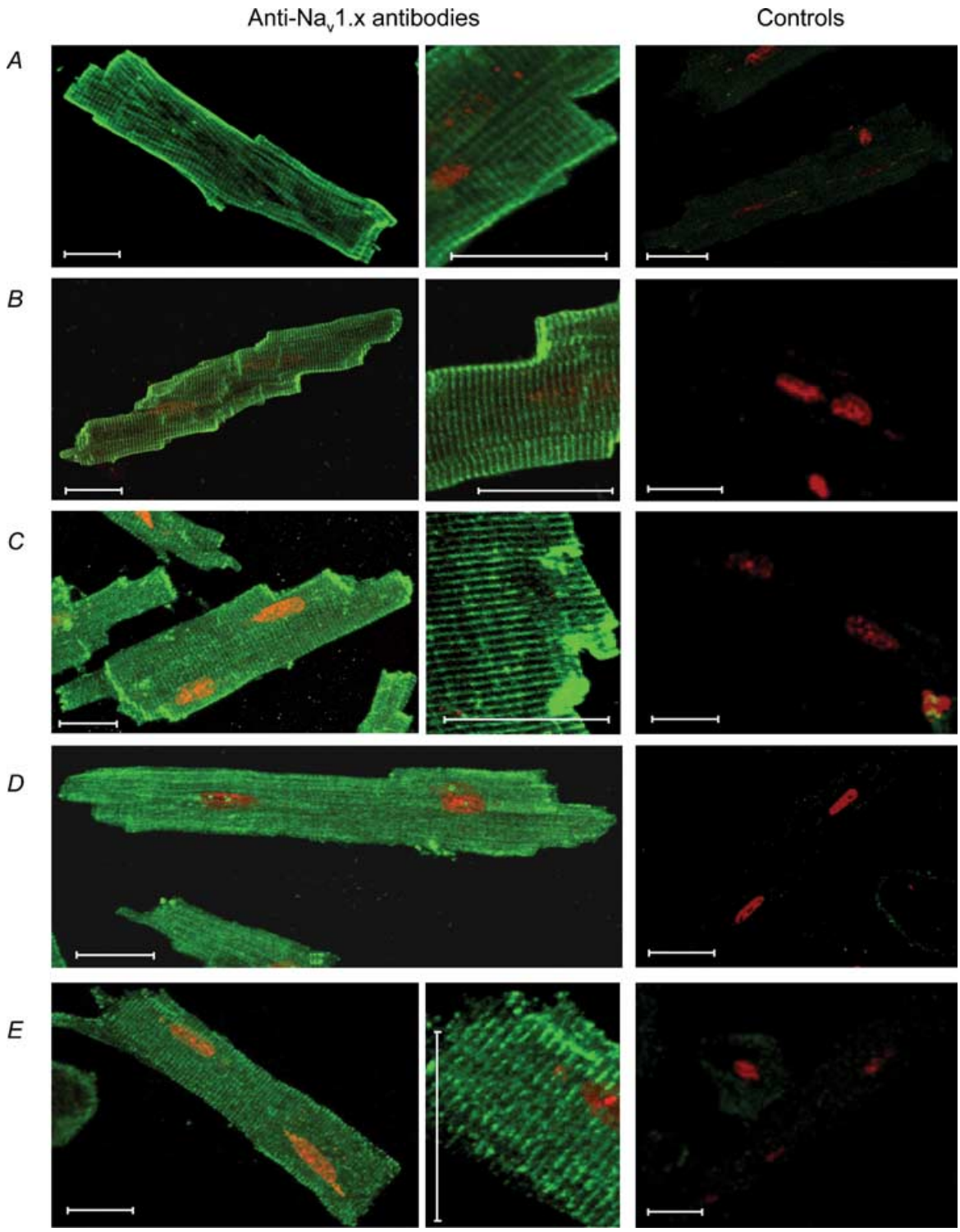

Figure 4. Cellular localization of Na^+ channel isoforms in mouse ventricular myocytes
The following primary antibodies were used: anti-$Na_v1.5$ (*A*), anti-$Na_v1.1$ (*B*), anti-$Na_v1.2$ (*C*), anti-$Na_v1.3$ (*D*) and anti-$Na_v1.6$ (*E*). Except for $Na_v1.3$ (*D*), cells are shown at a higher magnification (middle). Staining at the cell-to-cell contact regions and along the Z lines suggests a channel localization at the intercalated disks and in the t tubular membrane system, respectively, as recently concluded from double labelling experiments with connexin 43 and α-actinin (Maier *et al.* 2004). As controls, we routinely applied antibodies preabsorbed against their respective antigen (*B*–*E*, right) or we omitted a primary antibody (*A*, right). Controls are shown at the same gain as the original images. Because of very strong fluorescent signals, laser power and detector gain was reduced to record $Na_v1.5$ images. Propidium iodine (red) was added to stain nucleotide-rich areas (nucleus). Images were reconstituted from 15 serial optical sections. Scale bars, 20 μm.

In addition to the $Na_v1.5$ variants, we detected considerable quantities of neuronal and skeletal muscle Na^+ channel transcripts in the adult mouse heart. Previous TTX binding studies indicated the absence of TTX- and saxitoxin (STX)-sensitive receptors in fetal and neonatal hearts, and the appearance of high-affinity STX and TTX receptors at later stages of development in cardiac protein extracts (Renaud *et al.* 1983; Rogart *et al.* 1989). Our observations are consistent with these findings, as we observed very low amounts of neuronal and skeletal muscle Na_v transcripts at E15 and P1 compared with $Na_v1.5a$ and $Na_v1.5$ mRNA. From P1 to P126, however, our data indicate a gradual, age-dependent increase in the contribution of $Na_v1.2$, $Na_v1.3$ and $Na_v1.4$ to the total amount of transcripts, suggesting that these channels may form the basis for the increase in high-affinity STX receptors previously reported (Renaud *et al.* 1983; Rogart *et al.* 1989). It is noteworthy to mention that Rogart *et al.* (1989) reported that adult cardiac tissue contains between 25 and 50% of high-affinity STX receptors. These values are in strikingly good agreement with our results showing 30% (real-time RT-PCR) and 39% (competitive PCR) contributions of neuronal Na^+ channel mRNA in whole-heart preparations.

When comparing transcript levels in the adult whole heart *versus* isolated cardiomyocytes (Table 3), we found that the $Na_v1.4$ mRNA content was similar or even higher in isolated myocytes than in the whole-heart preparations, suggesting that $Na_v1.4$ is mostly distributed in the ventricles. In this context, it is noteworthy to mention that paramyotonia congenita, a disease caused by mutations in $Na_v1.4$, has been linked to prolongation of the QT interval on the ECG, a known arrhythmogenic substrate (Pereon *et al.* 2003), thus supporting the idea that $Na_v1.4$ channels contribute to ventricular electrophysiology.

On the other hand, neuronal Na^+ channel transcripts were less abundant in isolated ventricular cardiomyocytes compared with the whole heart. We suggest that this discrepancy is not simply due to high expression of these channels in other cardiac tissue types such as cardiac neurones or blood vessels, but mainly due to expression gradients within the myocardium. This conclusion is based on the following observations. First, blood vessels do not contain significant levels of neuronal Na^+ channel transcripts. Pereon *et al.* (2003) found $Na_v1.4$, $Na_v1.5$ and $Na_v1.6$ transcripts by RT-PCR in different regions of a human heart, but they did not detect these transcripts in the aorta. Moreover, peripheral vasodilatation upon *in vivo* application of TTX is exclusively due to the action of the drug on nerve fibres innervating blood vessels (Kao, 1966; Feinstein & Paimre, 1968). Second, our data on PGP 9.5, ENO2 and Na^+ channel transcript levels strongly suggest that cardiac nerve fibres are most likely not to be the origin of the relative high levels of $Na_v1.2$ and $Na_v1.3$ transcripts in the whole heart. Third, the heterogeneous distribution of Na^+ channel isoforms that we report in this study is consistent with a recent study (Haufe *et al.* 2005) that demonstrated much higher relative levels of $Na_v1.1$ and $Na_v1.2$ transcripts in dog Purkinje fibres than in ventricular cardiomyocytes, and an enhanced expression of $Na_v1.3$ in atrial cells. Furthermore, $Na_v1.1$ is highly

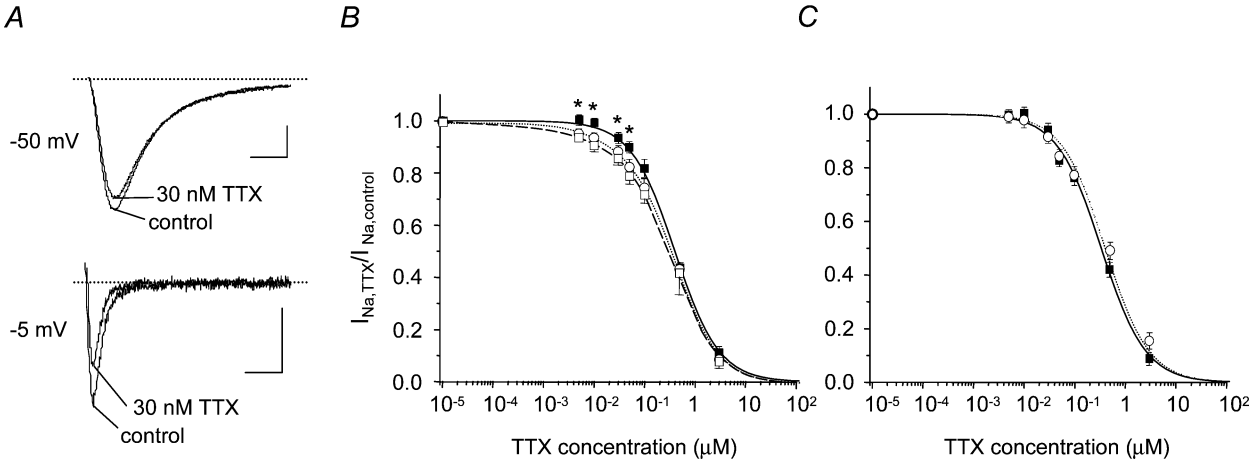

Figure 5. Detection of functional TTX-sensitive Na^+ channels in mouse cardiomyocytes by the whole-cell patch-clamp technique

A, representative current traces measured in an isolated cardiomyocyte at −50 and −5 mV in the absence and presence of 30 nM TTX (holding potential at −120 mV). Calibration bars, 2 ms and 1 nA. *B*, TTX blocking curve of isolated cardiomyocytes at the test potentials of −50 mV (■) and −5 mV (○, all cells; □, TTX-sensitive cells). Student's *t* test was used to test for statistical significance. The respective data points including the *P* values are shown in Table 5. $^*P < 0.05$. Bars represent means ± S.E.M. *C*, control experiments in HEK293 cells transfected with $mNa_v1.5$ ($n = 9$–18 for each concentration). Data points at the two test potentials were not significantly different.

Table 5. Block of TTX-sensitive Na^+ channels in mouse ventricular cardiomyocytes

	Mean Na^+ current fraction at				
TTX (nM)	−50 mV (all cells)	−5 mV (all cells)	−5 mV (TTXs cells)	*n*	*P* value
5	0.99 ± 0.01	0.95 ± 0.01	0.94 ± 0.01	24/17	0.002/0.001
10	0.98 ± 0.01	0.94 ± 0.02	0.91 ± 0.02	22/17	0.012/0.001
30	0.93 ± 0.01	0.89 ± 0.02	0.86 ± 0.02	21/14	0.033/0.009
50	0.90 ± 0.02	0.82 ± 0.03	0.79 ± 0.03	16/11	0.023/0.004
100	0.81 ± 0.04	0.74 ± 0.03	0.73 ± 0.02	12/8	0.124/0.100

Mean Na^+ current fractions, number of measurements (*n*) and *P* values (−5 mV *versus* −50 mV) are indicated both for all cells investigated, and for those cells only that showed a clearly detectable TTX-sensitive response (TTXs cells). Developmental stage: between postnatal days 35–50. Na^+ current data are presented as means ± S.E.M.

expressed throughout the murine sinoatrial (SA) node (Baruscotti *et al.* 1997; Maier *et al.* 2003; Lei *et al.* 2004). This neuronal isoform seems to be involved in SA node pacemaking in mice, thus contributing to the high heart rate of small rodents. In this context it is interesting to note that Na^+ channel expression gradients can be observed even within the highly specialized murine SA node: $Na_v1.5$ is not expressed in small SA node cells and in the region of the SA node located in the intercaval region (the centre of the SA node), but present in peripheral SA node cells (Lei *et al.* 2004).

In isolated ventricular cardiomyocytes, we detected functional TTX-sensitive Na^+ channels that are activated at more depolarized potentials compared with $Na_v1.5$ channels. These TTX-sensitive channels contributed to 8% to the transient Na^+ inward current (average value of all cells investigated). The corresponding RNA fraction was 15.6%. This discrepancy could be explained as follows. First, it seems that not all neuronal channels are properly integrated into the plasma membrane. Our immunofluorescence data strongly suggest that $Na_v1.3$, accounting for 3.6% of the pool of heart Na^+ channel transcripts (Table 3), is not expressed at the surface of ventricular myocytes. Second, alternative splicing may lead to nonfunctional channels, i.e. cells may possess the ability to adjust the amplitude of the TTX-sensitive I_{Na} to the actual metabolic needs by regulating the ratio of functional *versus* nonfunctional Na^+ channel transcripts. Third, the translation or trafficking efficiency, as well as the turnover rates for the different channel proteins, may vary considerably among the different isoforms. Considering $Na_v1.1$, we observed low transcript levels but strong fluorescence signals when labelling ventricular cardiomyocytes with a specific antibody. Although immunofluorescence is a nonquantitative method, this result suggests an efficient translation machinery for $Na_v1.1$. Fourth, the TTX-sensitive Na^+ channels may not be accessible for the electrophysiological measurements. It is possible that TTX-sensitive channels are located within caveolae, and can thus not be activated by the test pulse. Furthermore, in isolated cardiomyocytes, Na^+ channels are no longer in contact with the extracellular matrix, a factor that could be crucial for Na^+ channel activity.

What could be the physiological consequences of the coexistence of TTX-sensitive and TTX-resistant channels in cardiac myocytes? Balati *et al.* (1998) compared endocardial cells, epicardial cells, midmyocardial (M) cells and cells from Purkinje fibres with respect to the action potential amplitude (APA), the maximal rate of rise of the action potential (V_{max}) and the action potential duration (APD_{90}). The authors found that Purkinje cells show considerably higher APA and V_{max} values. TTX-sensitive Na^+ channels activate at more depolarized potentials and, therefore, may contribute to this phenomenon. This hypothesis is in good agreement with recent observations in dog that Purkinje cells contain high levels of TTX-sensitive Na^+ channel transcripts (Haufe *et al.* 2005). Moreover, action potentials are considerably longer in Purkinje cells (Balati *et al.* 1998) and already low doses of TTX significantly shorten the action potential duration in these cells (Coraboeuf *et al.* 1979). Although less pronounced, similar effects were also observed in ventricular M cells (Balati *et al.* 1998). These data strongly suggest that even a small fraction of TTX-sensitive Na^+ channels may produce a physiologically significant persistent Na^+ current that creates the action potential prolongation of these cells. A similar effect of TTX on the action potential duration was not observed in epicardial and endocardial cells (Balati *et al.* 1998), suggesting a pronounced heterogeneity among ventricular heart cells regarding the expression of TTX-sensitive Na^+ channels. In the present study, both real-time PCR (Table 3) and electrophysiological measurements (Fig. 5) revealed a respective cell-to-cell variability.

Our immunofluorescence results and data by Cohen (1996) are in contrast to data by Maier *et al.* (2002, 2004) who localized $Na_v1.5$ only at the intercalated disks, did not detect $Na_v1.2$, and found $Na_v1.1$ and $Na_v1.3$ distributed exclusively at the Z lines. Consequently, our data do not support the idea of Maier *et al.* (2002) that $Na_v1.5$ is specifically responsible for a saltatory-like mechanism of conduction, and that $Na_v1.1$ and $Na_v1.3$

are only involved in excitation–contraction coupling. The reasons for the discrepancies between our results and Maier *et al.* (2002, 2004) data remain unclear. Interpretation of immunohistochemical data regarding the exact membrane localization is in general difficult because of a number of potential problems (low cell quality, overload of the cells with primary antibody, reduced antibody accessibility, membrane folding at the intercalated disks, *xy* resolution of the laser scanning microscope leading to a high 'brightness factor' for t tubules; Blaustein & Lederer, 1999; Brette & Orchard, 2003). Because antibodies preabsorbed against their antigen did not yield fluorescence above background, we conclude that all four neuronal Na^+ channel proteins including $Na_v1.2$ are present in adult ventricular cardiomyocytes. $Na_v1.5$ channels were uniformly distributed in the plasma membrane at the intercalated disks and the t tubular membrane system, as suggested by the staining of cell-to-cell contact regions and along the Z lines, respectively. Na^+ channels at the intercalated disks may act as current amplifiers (Cohen, 1996) by establishing cleft potentials (Kucera *et al.* 2002) to improve cell-to-cell conduction, a mechanism reminiscent of saltatory conduction in neurones. Since we found a similar cellular localization for $Na_v1.5$, $Na_v1.1$ and $Na_v1.2$, we speculate also that these neuronal channels act in a similar fashion and help to maintain intraventricular conduction. In contrast to $Na_v1.1$ and $Na_v1.2$, $Na_v1.3$ was predominantly localized in intracellular compartments and seemed almost absent from the plasma membrane, which would exclude a contribution of most $Na_v1.3$ channel proteins to I_{Na}. Our results on $Na_v1.1$, $Na_v1.2$, $Na_v1.3$ and $Na_v1.5$ in mouse are similar to recent immunofluorescence data in dog ventricular cardiomyocytes (Haufe *et al.* 2004, 2005).

In conclusion, the present study indicates that a specific subset of Na^+ channels are differentially expressed in the heart at different developmental stages, and that neuronal Na^+ channels may play an important role in cardiac excitation and conduction. The requirements for neuronal Na^+ channels in the heart, and the physiological conditions under which they contribute to cardiac electrophysiology, remain elusive. By identifying and localizing the Na_v isoforms present in the heart, our study provides a basis for further studies of the physiological role of these channels in cardiac function based on their distribution and gating characteristics. Such study may become important in the context of cardiac arrhythmias linked to neuronal or musculoskeletal diseases or drug interactions.

References

Auld VJ, Goldin AL, Krafte DS, Marshall J, Dunn JM, Catterall WA, Lester HA, Davidson N & Dunn RJ (1988). A rat brain Na^+ channel α subunit with novel gating properties. *Neuron* **1**, 449–461.

Balati B, Varro A & Papp JG (1998). Comparison of the cellular electrophysiological characteristics of canine left ventricular epicardium, M cells, endocardium and Purkinje fibres. *Acta Physiol Scand* **164**, 181–190.

Balser JR (2001). The cardiac sodium channel: gating, function and molecular pharmacology. *J Mol Cell Cardiol* **33**, 599–613.

Baruscotti M, Westenbroek R, Catterall WA, DiFrancesco D & Robinson RB (1997). The newborn rabbit sino–atrial node expresses a neuronal type-I-like Na^+ channel. *J Physiol* **498**, 641–648.

Benndorf K (1993). Multiple levels of native cardiac Na^+ channels at elevated temperature measured with high-bandwidth/low-noise patch clamp. *Pflugers Arch* **422**, 506–515.

Benndorf K, Boldt W & Nilius B (1985). Sodium current in single myocardial mouse cells. *Pflugers Arch* **404**, 190–196.

Blaustein MP & Lederer WJ (1999). Sodium/calcium exchange: its physiological implications. *Physiol Rev* **79**, 763–854.

Brette F & Orchard C (2003). T-tubule function in mammalian cardiac myocytes. *Circ Res* **92**, 1182–1192.

Catterall WA (1992). Cellular and molecular biology of voltage-gated sodium channels. *Physiol Rev* **72**, S15–S48.

Chahine M, Deschene I, Chen LQ & Kallen RG (1996). Electrophysiological characteristics of cloned skeletal and cardiac muscle sodium channels. *Am J Physiol Heart Circ Physiol* **40**, H498–506.

Chomczynski P & Sacchi N (1987). Single-step method of RNA isolation by acid guanidinium thiocyanate–phenol–chloroform extraction. *Anal Biochem* **162**, 156–159.

Cohen SA (1996). Immunocytochemical localization of rH1 sodium channel in adult rat heart atria and ventricle. Presence in terminal intercalated disks. *Circulation* **94**, 3083–3086.

Coraboeuf E, Deroubaix E & Coulombe A (1979). Effect of tetrodotoxin on action potentials of the conducting system in the dog heart. *Am J Physiol Heart Circ Physiol* **236**, H561–567.

Cribbs LL, Satin J, Fozzard HA & Rogart RB (1990). Functional expression of the rat heart INa^+ channel isoform. Demonstration of properties characteristic of native cardiac Na^+ channels. *FEBS Lett* **275**, 195–200.

Day IN (1992). Enolases and PGP 9.5 as tissue-specific markers. *Biochem Soc Trans* **20**, 637–642.

Dib-Hajj SD & Waxman SG (1995). Genes encoding the $\beta 1$ subunit of voltage-dependent. Na^+ channel in rat, mouse and human contain conserved introns. *FEBS Lett* **377**, 485–488.

Feinstein MB & Paimre M (1968). Mechanism of cardiovascular action of tetrodotoxin in the cat. *Circ Res* **23**, 553–565.

Goldin AL (2001). Resurgence of sodium channel research. *Annu Rev Physiol* **63**, 871–894.

Haufe V, Cordeiro JM, Zimmer T, Wu YS, Schiccitano S, Benndorf K & Dumaine R (2005). Contribution of neuronal sodium channels to the cardiac fast sodium current I_{Na} is greater in dog heart Purkinje fibers than in ventricles. *Cardiovasc Res* **65**, 117–127.

Haufe V, Dumaine R, Benndorf K & Zimmer T (2004). Developmental expression patterns and immunolocalization of voltage-gated sodium channels in the mammalian heart. *Eur J Appl Physiol* **447** (suppl. 1), O13-6.

Heathers GP, Yamada KA, Kanter EM & Corr PB (1987). Long-chain acylcarnitines mediate the hypoxia-induced increase in alpha-1 adrenergic receptors on adult canine myocytes. *Circ Res* **61**, 735–746.

Huang B, El-Sherif T, Gidh-Jain M, Qin D & El-Sherif N (2001). Alterations of sodium channel kinetics and gene expression in the postinfarction remodeled myocardium. *J Cardiovasc Electrophysiol* **12**, 218–225.

Kao CY (1966). Tetrodotoxin, saxitoxin and their significance in the study of excitation phenomena. *Pharmacol Rev* **18**, 997–1049.

Kucera JP, Rohr S & Rudy Y (2002). Localization of sodium channels in intercalated disks modulates cardiac conduction. *Circ Res* **91**, 1176–1182.

Lei M, Jones SA, Liu J, Lancaster MK, Fung SS-M, Dobrzynski H, Camelliti P, Maier SKG, Noble D & Boyett MR (2004). Requirement of neuronal- and cardiac-type sodium channels for murine sinoatrial node pacemaking. *J Physiol 559* **3**, 835–848.

Maier SKG, Westenbroek RE, McCormick KA, Curtis R, Scheuer T & Caterall WA (2004). Distinct subcellular localization of different sodium channel α and β subunits in single ventricular myocytes from mouse heart. *Circulation* **109**, 1421–1427.

Maier SKG, Westenbroek RE, Schenkman KA, Feigl EO, Scheuer T & Catterall WA (2002). An unexpected role for brain-type sodium channels in coupling of cell surface depolarization to contraction in the heart. *Proc Natl Acad Sci U S A* **99**, 4073–4078.

Maier SKG, Westenbroek RE, Yamanushi TT, Dobrzynski H, Boyett MR, Catterall WA & Scheuer T (2003). An unexpected requirement for brain-type sodium channels for control of heart rate in the mouse sinoatrial node. *Proc Natl Acad Sci U S A* **100**, 3507–3512.

Malhotra JD, Chen C, Rivolta I, Abriel H, Malhotra R, Mattei LN, Brosius FC, Kass RS & Isom LL (2001). Characterization of sodium channel α- and β-subunits in rat and mouse cardiac myocytes. *Circulation* **103**, 1303–1310.

Mathy NL, Lee RP & Walker J (1996). Removal of RT-PCR inhibitors from RNA extracts of tissues. *Biotechniques* **21**, 770–774.

Nuss HB, Chiamvimonvat N, Perez-Garcia MT, Tomaselli GF & Marban E (1995). Functional association of the β_1 subunit with human cardiac (hH1) and rat skeletal muscle (μ1) sodium channel α subunits expressed in *Xenopus* oocytes. *J Gen Physiol* **106**, 1171–1191.

Pereon Y, Lande G, Demolombe S, Nguyen The Tich S, Sternberg D, Le Marec H & David A (2003). Paramyotonia congenita with an SCN4A mutation affecting cardiac repolarization. *Neurology* **60**, 340–342.

Renaud JF, Kazazoglou T, Lombet A, Chicheportiche R, Jaimovich E, Romey G & Lazdunski M (1983). The Na^+ channel in mammalian cardiac cells. Two kinds of tetrodotoxin receptors in rat heart membranes. *J Biol Chem* **258**, 8799–8805.

Rogart RB, Cribbs LL, Muglia LK, Kephart DD & Kaiser MW (1989). Molecular cloning of a putative tetrodotoxin-resistant rat heart Na^+ channel isoform. *Proc Natl Acad Sci U S A* **86**, 8170–8174.

Satin J, Kyle JW, Chen M, Rogart RB & Fozzard HA (1992). The cloned cardiac Na^+ channel α-subunit expressed in *Xenopus* oocytes show gating and blocking properties of native channels. *J Membr Biol* **130**, 11–22.

Schaller KL, Krzemien DM, McKenna NM & Caldwell JH (1992). Alternatively spliced sodium channel transcripts in brain and muscle. *J Neurosci* **12**, 1370–1381.

Sills MN, Xu YC, Baracchini E, Goodman RH, Cooperman SS, Mandel G & Chien KR (1989). Expression of diverse Na^+ channel messenger RNAs in rat myocardium. Evidence for a cardiac-specific Na^+ channel. *J Clin Invest* **84**, 331–336.

Smith RD & Goldin AL (1998). Functional analysis of the rat I sodium channel in *Xenopus* oocytes. *J Neurosci* **18**, 811–820.

Yu FH, Westenbroek RE, Silos-Santiago I, McCormick KA, Lawson D, Ge P, Ferriera H, Lilly J, DiStefano PS, Catterall WA, Scheuer T & Curtis R (2003). Sodium channel β4, a new disulfide-linked auxiliary subunit with similarity to β2. *J Neurosci* **23**, 7577–7585.

Zacharias DA, Garamszegi N & Strehler EE (1994). Characterization of persistent artifacts resulting from RT-PCR of alternatively spliced mRNAs. *Biotechniques* **17**, 652–655.

Zimmer T, Biskup C, Dugarmaa S, Vogel F, Steinbis M, Böhle T, Wu YS, Dumaine R & Benndorf K (2002*a*). Functional expression of GFP-linked human heart sodium channel (hH1) and subcellular localization of the α subunit in HEK293 cells and dog cardiac myocytes. *J Membr Biol* **186**, 1–12.

Zimmer T, Bollensdorff C, Haufe V, Birch-Hirschfeld E & Benndorf K (2002*b*). Mouse heart Na^+ channels: primary structure and function of two isoforms and alternatively spliced variants. *Am J Physiol Heart Circ Physiol* **282**, H1007–1017.

Acknowledgements

The authors would like to thank Dr H.-G. Schaible for helpful discussions, and K. Schoknecht and S. Bernhardt for excellent technical assistance. This work was supported by DFG grant Be1250/9–2 to K.B. and T.Z., grant NHLB number HL59449 to R.D., and BMBF grant 01ZZ0105/IZKF Jena to T.Z.

Author's present address

Robert Dumaine: Dépt. de Physiologie et Biophysique, Fac. de Médecine, U. de Sherbrooke, 3100 12th Avenue N., Sherbrooke Qc, Canada J1H 5N4.

Supplementary material

The online version of this paper can be accessed at:
DOI: 10.1113/jphysiol.2004.079681
http://jp.physoc.org/cgi/content/full/jphysiol.2004.079681/DC1 and contains supplementary material consisting of a figure entitled: Control PCR experiments for Nav1.4/Nav1.5 amplification using primer pair A5.
This material can also be found at:
http://www.blackwellpublishing.com/products/journals/suppmat/tjp/tjp843/tjp843sm.htm